Improved prediction of hydraulic conductivity for coarse-grained, unconsolidated material from nuclear magnetic resonance

Raphael Dlugosch[1], Thomas Günther[1], Mike Müller-Petke[1], and Ugur Yaramanci[2]

ABSTRACT

The prediction of hydraulic conductivity K from nuclear magnetic resonance (NMR) measurements has been performed primarily in sandstones. In hydrogeological applications, however, unconsolidated material is more prevalent. Compared to sandstones, unconsolidated sediments can show pore sizes up to several millimeters. The known (semi-)empiric relations to estimate K from NMR have been applied on this material, but the underlying assumptions are not valid for large pores. We formulated a new model, called the Kozeny-Godefroy model. It is based on capillary pores with a single pore radius, and accounts for bulk water relaxation and relaxation in porous media under fast- and slow-diffusion conditions. The bulk-water relaxation and slow-diffusion conditions significantly affect the NMR measurements on coarse material. If the impact of the bulk-water relaxation is well known and small, a maximum K can be derived from NMR measurements by accounting for the slow-diffusion case. The model replaces the empirical factors in known relations with physical, structural, and intrinsic NMR parameters. Focusing the calibration on material-specific NMR parameters improves the prediction of K for similar material. Measurements on well-sorted glass beads and natural sands with different grain sizes are used for evaluation. These measurements confirm the applicability of the new model and, for coarse material, show the limit of the fast-diffusion-based Seevers and Schlumberger-Doll-Research equations. The application of our model is limited to (1) simple pore geometries, and (2) materials with a small range of pore sizes.

INTRODUCTION

Permeability k, as a measure of the ability of a porous medium to transmit fluids, is a fundamental property. It is highly complex and, among other things, depends on the cross section dimensions of its flow channels and the saturation of the material. In hydrogeological applications, k is often replaced by the hydraulic conductivity (K), which integrates the fluid properties' viscosity and density, and therefore describes the ease of water to move through the pore space. The prediction of K is an important task in hydrology, and it is fundamental for aquifer characterization and hydraulic modeling. The Kozeny-Carman equation (Kozeny, 1927; Carman, 1938) is very popular and discussed in detail, e.g., by Carrier (2003). For fully saturated conditions, it relates k to the surface-to-volume ratio of tube-shaped flow channels.

For the prediction of k or K from geophysical measurements, the method of nuclear magnetic resonance (NMR) has proved to be very effective as shown, e.g., by Kenyon (1997). NMR can be applied in the laboratory, in the borehole, and from the earth's surface. The measured exponential relaxation signals (with relaxation times T_1 and T_2) are the result of the interaction of protons in the fluid with each other and with the matrix at the pore surface. This allows relating the relaxation time T (s) to the specific inner surface, i.e., the ratio of the inner surface per volume of the pores. The amplitude of the NMR signal is directly proportional to water content and therefore porosity (Φ) in case of full saturation. There are several (semi-)empiric formulas available to predict k from Φ and T. Among others, the popular equations are those from Seevers (1966) and Kenyon et al. (1988). The latter is commonly used in rock physics and is known as the Schlumberger-Doll-Research

(SDR) equation. Although these equations are established for sandstones, they may to some extent be used in shales (Josh et al., 2012), limestones (Akbar et al., 1995), and poorly consolidated reservoir sands (Kleinberg et al., 2003).

For many hydrological applications in the near subsurface, the properties of unconsolidated sediments are of particular interest. In contrast to sandstones, unconsolidated sediments may show pore sizes up to several millimeters. The assumption of fast diffusion (Brownstein and Tarr, 1979), which states that the selfdiffusion of the protons is fast enough that the whole pore is sampled during the relaxation process, may not be appropriate for such large pores. Thus, the equations of Seevers (1966) and Kenyon et al. (1988), which are based on this assumption, need to be revised. To predict k, both equations need a calibration constant (C) which is estimated, e.g., using flow experiments on samples in the laboratory. This constant C merges matrix parameters, such as tortuosity, and intrinsic material-specific NMR parameters. Converting these equations to estimate K (e.g., Legchenko et al., 2002), which is more common in hydrological applications, even highly temperature-dependent fluid parameters such as dynamic viscosity are merged into C.

In this work, we combine the Kozeny-Carman equation for hydraulic flow in tube-shaped pores and NMR relaxation times prediction as presented by Godefroy et al. (2001b) to a physical model called the Kozeny-Godefroy model (KGM). The model implements slow diffusion, accounts for bulk water relaxation, and directly implements matrix parameters as well as temperature-dependent fluid parameters.

In the following sections, we first give a review of the theory of how to predict hydraulic conductivities and how to link them to NMR measurements. This includes an overview of the commonly used equations and their derivations. Next, we present KGM and discuss the impact of the used model parameters. We evaluate our model by data measured on well-sorted glass beads and quartz sand with grain sizes ranging from fine sand to fine gravel. Finally, we compare KGM to the commonly used SDR and Seevers equations and discuss its limitations.

REVIEW OF THEORY

The Kozeny-Carman equation

To predict the permeability k (m^2) of an unconsolidated sample, the equation of Kozeny (1927) and Carman (1938) can be applied (e.g., Carrier, 2003). The equation is based on a simple model of parallel tube shape pores with a radius r_{tube} (m). Including a modification to estimate k (e.g., after Pape et al., 2006) the Kozeny-Carman equation is given by

$$k_{KC} = \frac{1}{8\tau^2} \Phi r_{tube}^2,$$ (1)

where τ is the (dimensionless) tortuosity and Φ the (dimensionless) ratio of void to total volume.

Equation 1 can be converted from the original description of tube-shape pores to other (matrix) geometries using an equivalent surface-to-volume ratio S/V (1/m). Assuming smooth and spherical grains with a diameter d_{grain} (m), simple geometric considerations lead to

$$r_{tube} = \frac{1}{3}\frac{\Phi}{1-\Phi}d_{grain},$$ (2)

which allows for estimating k based on sieving analyses. We use the effective grain diameter after Carrier (2003),

$$d_{grain} = 1/\sum \frac{f_i}{d_{li}^{0.5} d_{si}^{0.5}},$$ (3)

where f_i is the (dimensionless) fraction of particles between the sieve-size d_{li} and d_{si} (m), which are the respective sieve sizes limits.

In hydrological application, k is often replaced by the hydraulic conductivity K (m/s), which integrates the fluid properties dynamic viscosity η (Pa s) and density ϱ (kg/m^3) under the gravity acceleration ($g = 9.81$ m/s^2). Under fully saturated conditions, K can be written as

$$K = \frac{\varrho g}{\eta}k.$$ (4)

Because of the primary hydrological application in unconsolidated material, we focus this work on the determination of K and adapt the following equations appropriately. Apart from the temperature-dependency of K due to η and ϱ (see Table 1), most results presented in this paper are equally true for k and can be transferred using equation 4.

NMR relaxation times

NMR takes advantage of the phenomenon that an ensemble of hydrogen protons exposed to a static magnetic field B_0 (T) exhibits a macroscopic magnetization M (A/m) in thermal equilibrium that is aligned with the direction of B_0. During an NMR experiment, electromagnetic pulses are used to rotate the direction of the magnetization by some angle. The return to equilibrium is described by the Bloch equation (Bloch, 1946). Solution of the Bloch equation yields two independent relaxation processes, one perpendicular, the other aligned with the static field, and both of exponential character. Accordingly, both are described by a time constant, the longitudinal relaxation time T_1 (s) for rebuilding the magnetization aligned with B_0, and the transverse relaxation time T_2 (s) for the collapse of the magnetization perpendicular to B_0.

Seevers (1966) describes the relaxation time T_1 by a sum of two processes: the bulk relaxation T_B (s) and a fast relaxation close to a grain surface

$$\frac{1}{T_1} = \frac{1}{T_B} + r_s \frac{V_S}{V_B}.$$ (5)

The relaxation rate r_s (1/s) characterizes the layer that is in contact with the grain surface, V_S (m^3) is the volume of water in this layer, and V_B (m^3) is the pore volume. This relation links the NMR signal to S/V of the pore and therefore gives rise to hydraulic properties. Note that T_B is controlled by the self-diffusion constant D (m^2/s) of water (Bloembergen et al., 1948). Because D again is a function of η (Krynicki et al., 1978), T_B and D are both temperature dependent. Additionally, T_B is influenced by the amount of dissolved oxygen and ferromagnetic and paramagnetic ions, such as iron or manganese (Bloembergen et al., 1948; Dunn et al., 2002). Therefore, T_B should be estimated directly on the extracted pore fluid and at the same temperature if possible.

Brownstein and Tarr (1979) introduce a simple diffusion model linking the measured relaxation times T_1 to pores with basic shapes including tubes with radius r_{tube}. The model contains the self-diffusion constant D of water and surface relaxivity ρ (m/s), but neglects T_B. The material-specific surface relaxivity ρ describes the interaction of the protons with the pore surface. The authors distinguish two limiting cases (fast diffusion and slow diffusion) depending on the dimensionless sink-strength parameter

$$B = \rho r_{\text{tube}}/D \tag{6}$$

and present an equation linking relaxation time to pore size separately for each case.

The equation for fast diffusion ($B \ll 1$) matches the formulation of Seevers (1966) (equation 5) without T_B. The dominant signal is the first-order solution of the governing differential equations, i.e., the main mode ($n = 0$). For a single water-filled pore, this results in a primarily monoexponential signal. If a certain pore size corresponds to a monoexponential signal, then a distribution of pore sizes within one sample will lead to a measured multiexponential signal, i.e., a distribution of relaxation times. Assuming a constant ρ, this leads to a linear relationship between pore size and relaxation time distribution. A logarithmic mean is commonly used to represent a T distribution (Dunn et al., 2002), i.e., to represent a sample by a mean pore size.

For the slow-diffusion case ($B \gg 10$), however, the relation between the relaxation time and the pore size changes. The observed NMR signal from a single pore becomes multiexponential due to the higher-order solutions. The relaxation times of these higher modes ($n > 0$) are significantly faster than the main mode and their amplitudes sum up to a significant amount of the total signal for increasing values of B. Consequently, in the case of slow diffusion, an NMR T distribution may not be related to a pore radius distribution. Thus, a logarithmic mean does not represent an mean pore size of a sample. The region of intermediate-diffusion ($1 \leq B \leq 10$) is not explicitly described by Brownstein and Tarr (1979).

While Brownstein and Tarr (1979) gave separate equations for slow and fast diffusion, Godefroy et al. (2001b) find a solution that describes the main mode ($n = 0$) for the complete range of B, by excluding very early times in the NMR relaxation, i.e., neglecting higher modes ($n > 0$)

$$\frac{1}{T_1} = \frac{1}{T_B} + \frac{1}{\frac{r_{\text{tube}}}{2\rho} + \frac{r_{\text{tube}}^2}{4D}}. \tag{7}$$

Obviously, using the relaxation time of the zeroth mode to estimate a pore radius is correct only if a single radius is present, i.e., a relaxation time distribution is due to higher modes and not due to a distribution of pore sizes.

In addition to the described processes, the relaxation time T_2 is influenced by the movement of the protons in a magnetic gradient field due to diffusion (Kleinberg and Horseld, 1990). However, this effect is usually neglected when using CPMG pulse sequences (Carr and Purcell, 1954; Meiboom and Gill, 1958) at low NMR frequency and short pulse spacing. Under these conditions, T_2 and T_1 yield identical pore size information (Kleinberg et al., 1993). We therefore refer the subsequent equations to T, which is valid for T_2 only under the described limitations, i.e., negligible magnetic field gradients. But, because $T_1 \geq T_2$, this leads to relaxation time specific ρ.

To estimate ρ of a sample, fast-diffusion conditions are usually assumed (e.g., Kenyon, 1997). The relaxation time T and the volume of the pores V are measured using NMR and the pore surface S is measured independently using different methods, e.g., section images (e.g., Straley et al., 1987), hydraulic conductivity (e.g., Kenyon et al., 1989), nitrogen adsorption, or NMR-diffusion measurements (e.g., Hürlimann et al., 1994). All of these methods have their individual sensitivities to the roughness of the pore surface, thus leading to a wide variation of S and ρ, up to a factor of 10 and more. Therefore, Kenyon (1997) introduces an effective or apparent surface relaxivity ρ_a when relating NMR to hydraulic measurements. Consequently, we use ρ_a for the samples presented in this study.

Hydraulic conductivity from NMR measurements

To predict k from NMR measurements, an analytic solution can be achieved by combining the Kozeny-Carman (equation 1) with equation 5 as presented by Seevers (1966). Including the fluid properties to predict K using equation 4 leads to the SB (Seevers including bulk relaxation) model,

$$K_{\text{SB}} = C_{\text{SB}} \Phi \left(\frac{T_B T}{T_B - T} \right)^2. \tag{8}$$

The same result can be achieved using Kozeny-Carman and the fast-diffusion approximation after Brownstein and Tarr (1979), comprising the matrix properties (ρ and τ) and fluid properties (ϱ, η, and g) in the constant $C_{\text{SB}} = (\varrho g \rho^2)/(2\eta\tau^2)$.

In analogy to Kozeny-Carman, but derived empirically, Kenyon et al. (1988) present the SDR equation to predict k from NMR measurements, which is based on several data sets measured on sandstones,

$$K_{\text{SDR}} = C_{\text{SDR}} \Phi^4 T^2. \tag{9}$$

SDR and SB comprise several parameters as pore geometry and surface relaxivity as well as temperature-dependent fluid parameters into the empirical factors C_{SB} and C_{SDR} (m/s^3). These factors are obtained from calibration measurements for each sandstone formation or material. Ranges for C_{SB} and C_{SDR} can be found in literature, for sandy material summarized, e.g., by Mohnke and Yaramanci

Table 1. Physical properties of water and their dependency from the temperature θ (°C). The equation for T_B was approximated by an empirical fit on continuous T_2 measurements during the warm up of tap water from 5°C to 35°C.

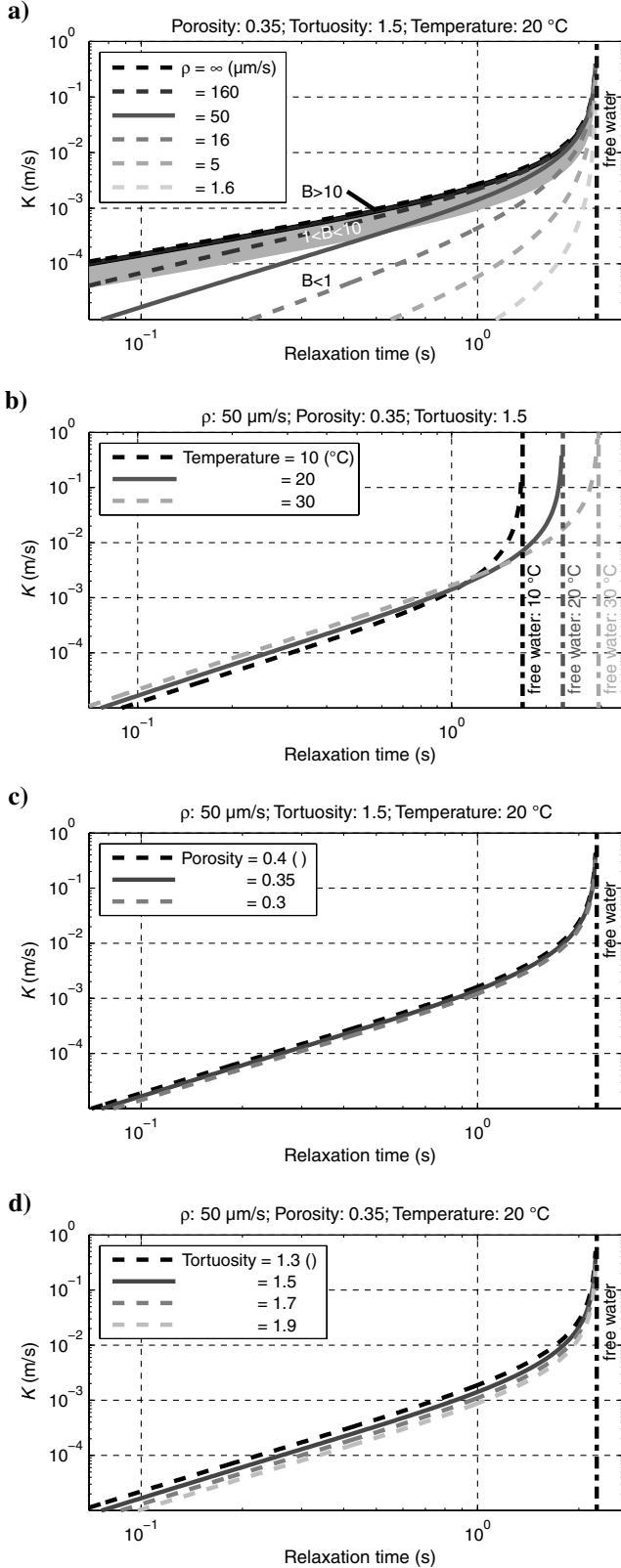| Parameter	Equation	Reference
T_B (s)	$3.3 + 0.044(\theta - 35)$	own T_2 measurements
η (Pa s)	$[1002, 797, 653] \cdot 10^{-6}$ for $\theta = [20, 30, 40]$	tabular (Kestin et al., 1978)
D (m^2/s)	$1.0413 + 0.039828\theta + 0.00040318\theta^2$	(Dunn et al., 2002)
ϱ (kg/m^3)	$1000(1 - \frac{\theta + 288.94}{508929(\theta + 68.12)}(\theta - 3.98)^2)$	(McCutcheon et al., 1993)

a)

b)

c)

d)

Figure 1. Sensitivity of KGM to variation of the model parameters surface relaxivity, temperature, porosity, and tortuosity (a-d). The default values are marked by continuous lines. Regions of inter-mediate ($1 \leq B \leq 10$) and slow diffusion ($B \leq 10$) are shaded (a).

(2008) to predict K for a temperature of 10°C. Due to the limitations or data sets used to estimate equations 8 and 9, we summarize them as fast-diffusion approximations.

Other semiempirical approaches have been published by Timur (1968) and Coates and Dumanoir (1973), which can also be traced back to the Kozeny-Carman equation. Due to the lack of bound water for the coarse and clay-free material of the presented samples, Timur-Coates-like equations cannot be applied successfully and are therefore not further discussed in this paper.

The presented SDR and SB differ (1) in the porosity exponent (four and one) and (2) by neglecting and accounting for bulk relaxation, respectively. Note that the porosity exponent is subject to discussion (Kenyon et al., 1988; Mavko and Nur, 1997). The presented samples in this work show minor variations of Φ. Thus, for the prediction of K for presented samples, the porosity exponent has an impact only on the calibration constant. Therefore, SDR and SB primarily differ due to the influence of T_B for long relaxation times.

KOZENY-GODEFROY MODEL

Derivation

To obtain a model to estimate K from NMR measurements on unconsolidated material, we combine Kozeny-Carman (equation 1) with Godefroy (equation 7), and convert them to K using equation 4. Note that the main requirements of Kozeny-Carman and Godefroy remain. The model is referred to as KGM,

$$K_{\text{KGM}} = \frac{\varrho g}{8\tau^2 \eta} \Phi \left(\frac{-D}{\rho} + \sqrt{\left(\frac{D}{\rho} \right)^2 + \frac{4DT_B T}{T_B - T}} \right)^2. \quad (10)$$

This allows to estimate K by (1) measuring Φ and T using NMR, (2) adapting T_B, η, D, and ϱ according to the sample temperature, and (3) calibrating ρ and τ or assuming values from literature. The sensitivity of KGM to its model parameters is discussed in the following.

Sensitivity to model parameters

The KGM (equation 10) depends on several model parameters. Some of them cannot be estimated by a simple NMR experiment but need to be chosen using additional information. Apart from g, they can be subdivided into sample or matrix specific parameters (ρ, Φ, τ) and fluid parameters (T_B, η, D, ϱ). To show their impact on KGM, we discuss them individually, while the variation of the fluid parameters are realized by temperature variation. As the default model, we chose $\rho = 50$ μm/s, $\Phi = 0.35$, $\tau = 1.5$, and a temperature of 20°C. These values are based on our observations and expectations for clay-free unconsolidated material and are referenced and discussed in more detail in the respective paragraph. The successive variation of one specific model parameter from the default model is presented in Figure 1.

First, we discuss the impact of the surface relaxivity on KGM (Figure 1a) and focus on the left part. For a given pore size, e.g., resulting in $K = 10^{-3}$ m/s, an increase in ρ has two effects: (1) The measured relaxation time T of the main mode is reduced and (2) the diffusion condition gradually changes from fast to slow diffusion. Neglecting the impact of T_B, the dependency of K from T changes from $K \propto T^2$ for the fast-diffusion case gradually to $K \propto T$ for the slow-diffusion case, where T is finally no longer

a function of ρ. This leads to a physical upper limit of K for a measured T and Φ. With increasing impact of T_B, i.e., for coarse material, T_B starts dominating T and therefore the estimation of K. Consequently, we need to evaluate the impact of T_B.

For a constant fluid chemistry, T_B is controlled by the temperature θ (°C). We used the temperature dependency for tap water (see Table 1) and focus on the temperature range between 10°C and 30°C (T_B between 2.2 and 3.1 s), typical for the laboratory and shallow field applications. Figure 1b shows that K of coarse material can be estimated reliably only if T_B is known. However, temperature variations basically change the fluid viscosity η. On the one hand, this change in η affects D, and therefore T_B and thus the NMR relaxation. For example, for lower temperatures, T_B is shifted to shorter relaxation times and D is reduced. Because smaller D values directly lead to a reduction of B, the fast-diffusion approximation can be violated and higher modes may occur in smaller pores. On the other hand, the viscosity change affects the macroscopic flow and therefore K. Nevertheless, temperature can be easily measured in the laboratory and borehole or approximated for field applications. Its impact on η, D, and T_B can either be gained from the literature or from separate measurements (e.g., see Table 1).

The expected range of porosity for unconsolidated, well-sorted, and clay-free material is rather small. Because KGM uses a tube-shaped pore model, porosity contributes linearly to K, thus leading to relatively small changes (Figure 1c). Under fully saturated conditions, Φ can be easily estimated from the amplitude of the NMR signal.

Similar to Φ, the expected range of tortuosity for clay-free and well-sorted unconsolidated material is small and leads to a small shift in K (Figure 1d). However, for higher values of τ, as, e.g., found on sandstones, its effect can become significant due to its quadratic term. For this study, a mean value of 1.5 was chosen that lies between $\pi/2$ after Bartell and Osterhof (1927) and $\sqrt{2}$ after Carman (1956). It is also in good agreement with Pape et al. (2006) who estimated $\tau = 1.5$ from NMR diffusion measurement on glass beads.

METHODS

Sample material and preparation

To be able to provide samples of homogeneous material and grain shape over a wide range of grain sizes (d_{grain} between 90 μm and 4.4 mm) we chose glass beads for evaluating the KGM. The beads (Sigmund Lindner GmbH, Warmensteinach, Germany) consist of soda lime glass with a chemical composition of mainly SiO_2: 54.7%, Al_2O_3: 14.5%, CaO: 22.5%, and B_2O_3: 5.5%. The particles are spherically shaped and split into samples with narrow grain-size ranges as shown in Table 2. Additionally, a set of sand samples with high quartz content (Euroquarz GmbH, Dorsten, Germany) but natural grain shape is used to show the applicability of KGM to predict K on natural material.

To be able to visually check the correct installation of the material, we used a lucent polycarbonate sample holder with a length of 110 mm and an inner diameter of 40 mm. The dimension was chosen to be big enough to hold a representative volume of the material but still fit in the coil of the used laboratory NMR.

The samples were saturated with degassed and deionized water to which sodium chloride was added to reach an electrical conductivity of 400 μS/cm. The sample holder was first filled with the fluid and then the grains were slowly added to the water column to prevent air pockets. The material was gradually filled and compacted with a pestle to achieve similar porosities.

Hydraulic conductivity measurements

To determine the hydraulic conductivity K_{meas} of the samples, the constant-head setup was applied. A fundamental assumption for this experiment is to maintain laminar flow conditions, which is a challenge for coarse material. Therefore, Reynolds numbers for flow in a tube and packed bed were estimated for each measurement. Additionally, the experiments were conducted with different flow rates and checked for consistency. The temperature of the fluid was measured and K_{meas} was corrected to a common temperature of 22°C using equation 4 to make K consistent with the thermal equilibrium reached during the NMR measurements. To estimate the error of K_{meas}, we used a quadratic propagation of uncertainty from all input parameters. The results were compared to K_{KC} (Figure 2) estimated from sieving analyses using the Kozeny-Carman equation to predict K (combining equations 1, 3, and 4) with $\tau = 1.5 \pm 0.1$. To estimate an error for K_{KC}, we used the range of geometric parameters d_{grain} and Φ measured on each sample. We observe a good agreement between K_{KC} and K_{meas} within their error levels which supports the use of the tube-shaped pore model for well-sorted, clay-free material. The small trend to overestimate K_{KC} might be

Table 2. List of the sample parameters: material, grain size, and porosity. Apparent surface relaxivity (ρ_a) and sink strength parameter (B) of the samples derived from KGM using the individual measured Φ, K_{meas}, and respective T_1 or T_2 values of each sample. The range of ρ_a and B is derived from the error range of the input parameters.

Material	d_{grain} (sieving) (μm)	Φ (NMR) ( )	ρ_a (T_2) (μm/s)	B (T_2) ( )	ρ_a (T_1) (μm/s)	B (T_1) ( )
Glass beads	4400–3600	0.39	∞ – 0	∞ – 6.0	∞ – 0	∞ – 0.2
	1650–1250	0.35	160–0	∞ – 1.5	160–0	11–0.7
	500–250	0.38	54–38	2.8–0.8	43–30	2.0–0.6
	150–90	0.37	66–55	0.9–0.4	42–35	0.6–0.2
Quartz sand	2000–630	0.41	297–0	13–0.9	232–0	13–0.2
	1000–500	0.38	73–20	11–1.1	74–18	13–1.0
	500–125	0.34	44–34	1.5–0.5	22–14	0.6–0.3
	250–63	0.40	41–31	0.6–0.2	37–30	0.6–0.2

due to an underestimation of S/V assuming spherical and smooth grains. An increase of τ to 1.7 might account for this. The value is within the expected effect of the shape factor for nonspherical grains as, e.g., reported by Carrier (2003).

NMR measurements

The NMR measurements were carried out using the Rock Core Analyzer (Magritek, Wellington, New Zealand) which operates at 2 MHz. We used the built-in cooling system to ensure a constant sample temperature between 21°C and 22°C during the measurements.

The T_1-relaxation was measured by an inversion recovery experiment using 50 logarithmically delays ranging from 0.01 to 15 s. To determine T_2, we used a CPMG pulse sequence with an echo spacing of 200 μs which we sampled logarithmically to 500 data points. To obtain a T_1 (T_2) distribution, we allowed for 150 (300) logarithmically spaced time bins from 0.01 to 10 s during the inversion.

Because T_B is not only a function of temperature, but can be altered by dissolved ions, we estimated T_B separately for every sample. Therefore, after the NMR experiments on the sample, we extracted the pore fluid and measured T_2 of the liquid.

Estimating a representative T or T-distribution of a sample is essential to conclude on hydraulic properties using NMR. Figure 3 shows an exemplary T_2-distribution derived by a smooth multiexponential fitting (see, e.g., Whittall et al., 1991). A regularization parameter λ is used to weight between minimum structure in the T-distribution and minimum residual between measured data and model response. For comparison, we show a single-pore mode (SPM) fit after Ronczka et al. (2012). The SPM approach calculates the first 10 modes of a single pore and adapts r_{tube} and ρ accordingly. Both smooth and SPM fit explain the data comparably well, and therefore show that modes may not be ignored for coarse material. Additionally, T of the main mode agrees well with the maximum of the smooth distribution. This supports the assumption that the presented sample can be described by a single pore radius whose information is comprised in the maximum of the smooth distribution.
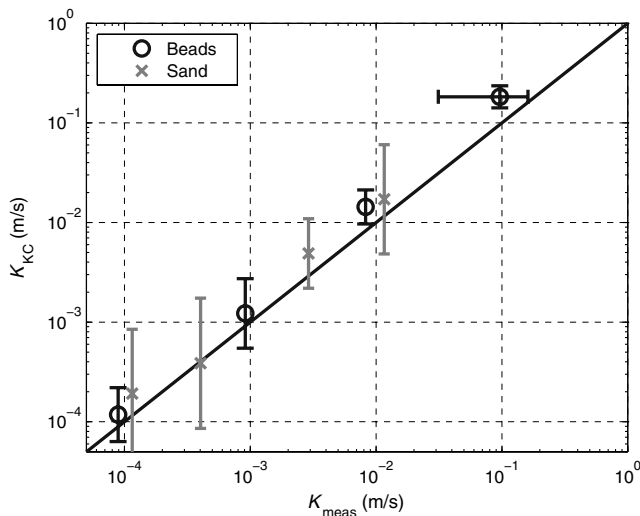
tribution. Therefore, we use this maximum in analogy to Godefroy et al. (2001a).

To estimate the error of the calculated T, we vary λ of the smooth inversion to estimate the range of T which sufficiently explains the measured data without leaving structure in the residual and significantly increasing the misfit above the noise level. For the samples presented in this work, the relative error of T is in the range of 0.05.

RESULTS

Evaluation of KGM

The results for the measured T_2 and K_{meas} on glass beads and sand are presented in Figure 4. Contour lines of KGM for a range of ρ from five to ∞ (μm/s), a fixed mean sample porosity of 0.38, and a fluid temperature of 22°C are plotted for comparison. The value of $T_B = 2.39$ s has been estimated by separated NMR measurement on all sample fluids. The two different sample types (sand and glass beads) line up on respective contour lines of constant ρ. This visual comparison is somehow limited because Figure 4 only shows a mean KGM. It does not account for variations of Φ for some samples of up to 0.03, and does not show the uncertainty of the KGM due to the used input parameters. The uncertainty of the KGM is mainly due to T_B, with an error of ±0.07 s estimated from extracted sample fluids, and τ with ±0.01 approximated from Φ variation after Lanfrey et al. (2010).

To overcome these limitations, we calculated the surface relaxivity for every sample by rearranging equation 10 to solve ρ and use the sample-specific values of Φ. However, dealing with real samples

Figure 2. Comparison of K of glass beads and quartz sand samples measured by flow experiment and predicted using the Kozeny-Carman equation. The black line marks the identity. Error bars smaller than marker size are not shown.
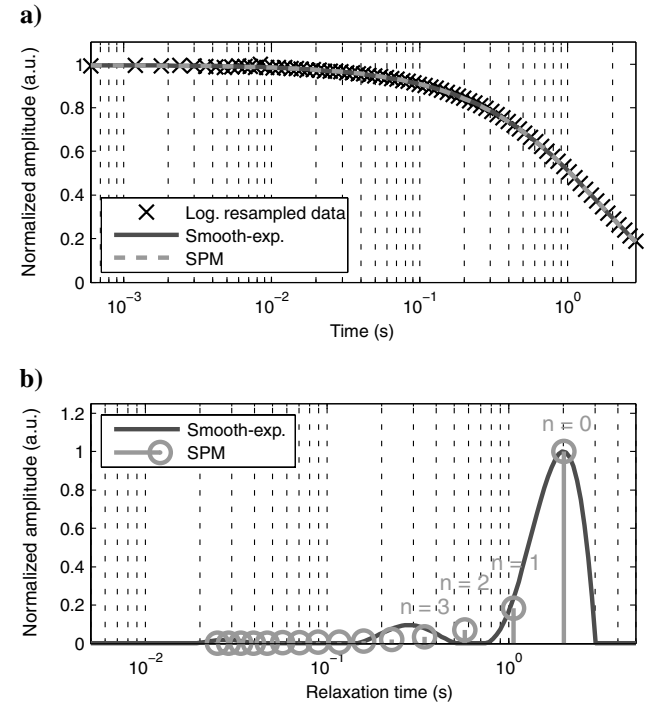

Figure 3. Logarithmically equidistant resampled T_2 relaxation curve of water-saturated glass beads with a grain size of 1250–1650 μm and fitted T-models with a smooth distribution and using SPM (a). Distribution of the fitted modes including the mode number n (b). RMS(smooth) $= 2.29 \times 10^{-4}$ and RMS(SPM) $= 2.35 \times 10^{-4}$.

with, for instance, unknown pore roughness, we refer to these values as apparent surface relaxivity ρ_a. The ranges of ρ_a, obtained by a quadratic propagation of uncertainty for all input parameters, are listed in Table 2. Examination of the value ranges suggest that 55 μm/s might be a reasonable value for ρ_a when applying T_2 measurements on glass beads. For sand, the respective ρ_a seems to be slightly lower (35 μm/s). For T_1, the respective ρ_a are ≈37 μm/s for glass beads and ≈30 μm/s for sand. These values are in the range of surface relaxivities found in the literature (see Table 3) when NMR diffusion measurements and section images are used to estimate *S*. The fact that the ρ for the glass beads presented by Godefroy et al. (2001b) are significantly lower might be due to the intense washing of the samples with hydrogen chloride, which was not conducted in this work.

DISCUSSION

KGM compared to Seevers and SDR

To evaluate if other models might also explain the measurements, we compare KGM (equation 10) with results obtained from SB (equation 8) and SDR (equation 9). The results are displayed in Figure 5. We use a T_B of 2.39 s and measurements of K_{meas}, Φ, and T_2 on the samples with smallest grain sizes to calibrate all equations by estimating a respective material specific ρ, C_{SB}, and C_{SDR}. This sample was chosen for calibration because it most likely fulfills the requirements where all equations are valid. For small values of *K* and *T*, the contour lines of all equations are in good agreement in shape ($K \propto T^2$) and value. But, using the calibrated equations to predict *K* of more coarse but similar material, SB and SDR are unable to explain the measured data. Under these conditions, two effects with opposed signs determine the relation between *T* and *K*.

One effect is due to T_B, which is, because Φ is constant, the only difference between SB and SDR. The bulk relaxation time limits *T* and leads to an underestimation of *K* if ignored. Its amplitude is a function of *T* and becomes increasingly important for high *T* values. Thus, a good knowledge of T_B is essential for NMR measurements on coarse material.

But the two facts, that (1) the measurements on the samples do not line up with SB, and (2) that they show a material-specific deviation from SB and SDR, is due to the violation of the fast-diffusion approximation dependent on *D* and ρ. Because KGM accounts for the limiting effect of *D*, which for larger pores leads to higher *T* values than expected by the fast-diffusion approximation, the measurements on samples with different grain sizes still line up on a single contour line of ρ. The deviation between the measurements on the samples and SB and SDR is, additionally, material specific. For SB, the deviation is larger for glass beads compared to sand. By estimating a material specific ρ value for KGM, the measurements again line up on a single contour line of ρ. To quantify the grain size where the fast-diffusion approximation is no longer appropriate for the presented samples, we calculated *B* for each sample using equation 6. Ranges of ρ_a are obtained from KGM (see Table 2) and r_{tube} are estimated from K_{meas} using equations 1 and 4. These values indicate that for grain sizes larger than approximately $d_{\mathrm{grain}} > 250$ μm, $B \ll 1$ is violated. Therefore, the fast-diffusion approximation, and in consequence the application of SB and SDR, is no longer valid.

Finally, the capabilities of KGM, SB, and SDR to predict *K* using the sample specific Φ are shown in Figure 6. The model parameters

and error ranges were estimated as described in the section results. All equations are calibrated on the sample with the smallest grain size of each data set, respectively, and are consequently used to predict *K* for more coarse material as described before. Apart from the violation of the requirement for SB and SDR, using coarse material for calibration is also not recommended for KGM because of the reduced resolution of ρ_a due to T_B (see Table 2). After this calibration, KGM is able to predict *K* from Φ and from T_2 and T_1 over the whole range of presented grain sizes from fine sand up to fine gravel. For the presented samples, SB and SDR show systematic deviations from the hydraulic measurements for coarse material which result in an overestimation of *K* using SB and an underestimation using SDR.

Limitation of the flow model

The presented KGM is developed and validated assuming fully water-saturated unconsolidated material and homogeneity at every scale. As summarized by Carrier (2003), the application of Kozeny-Carman-type equations is limited to laminar flow, not-too-wide
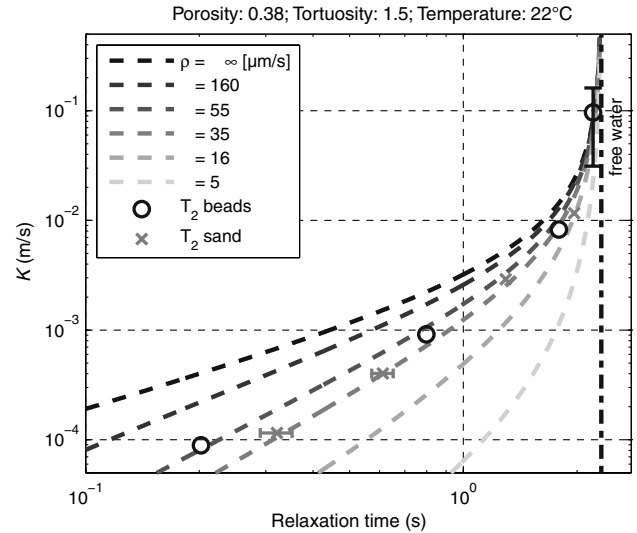
Figure 4. KGM for a porosity of 0.38, T_B of 2.39 s, a temperature of 22°C, and varying surface relaxivity. The T_2 relaxation times and K_{meas} measured on glass beads and quartz sand samples with different grain sizes. Error bars smaller marker size are not shown.

Table 3. References for ρ estimated from T_1 and *S* measurements assuming fast-diffusion conditions. The method used to estimate *S* as well as different sample materials are listed.

Sample	Methods for *S*	ρ (μm/s)	Reference
Sandstones	NMR diffusion	2.6–40	(Hürlimann et al., 1994)
Sandstones	Section images	10–60	(Kenyon et al., 1989)
Sandstones	Section images	30–300	(Howard et al., 1993)
Glass beads	Section images	11.5	(Straley et al., 1987)

grain size distribution, noncompact particle shapes, and no electrochemical reactions. The latter is why clayey material is not covered.

A tube-shaped pore model sufficiently explains the presented data set of K measured on sand and glass beads using a theoretically derived τ of 1.5 (see Figure 2). However, real pores do generally not fit the assumptions of simplified pore geometries and smooth surfaces. To account for the impact of the deviation on K, τ can be adjusted accordingly. A change of τ to 1.7 slightly improves the prediction of K for the presented samples from the Kozeny-Carman equation by reducing K_{KC}. This change in τ leads to an increase of ρ_a obtained from KGM by a factor of approximately 1.3. More complex pore models may also explain the measured data, but no analytic solutions of the governing equations are given for more complex geometries. Other analytic solutions for planar and spherical pore geometries are given in Appendix A.

Limitation of the NMR model

The samples presented in this work were chosen to show a small grain-size distribution to avoid the ambiguity that multiexponential signals either arise from different pore sizes or higher modes. Using the maximum of the T-distribution allows to find an adequate measure for a sample with a single-pore radius in the slow- and fast-diffusion cases. If a material with a wide distribution of pore radii is present, using only the maximum of the T-distribution will result in ignoring the effect of pores which are not represented by this maximum. Ignoring small/large pores will result in an over-/underestimation of T and thus K. A common approach in SDR handling wide distributions uses the logarithmic mean for T. Note that this is appropriate only under fast-diffusion conditions.
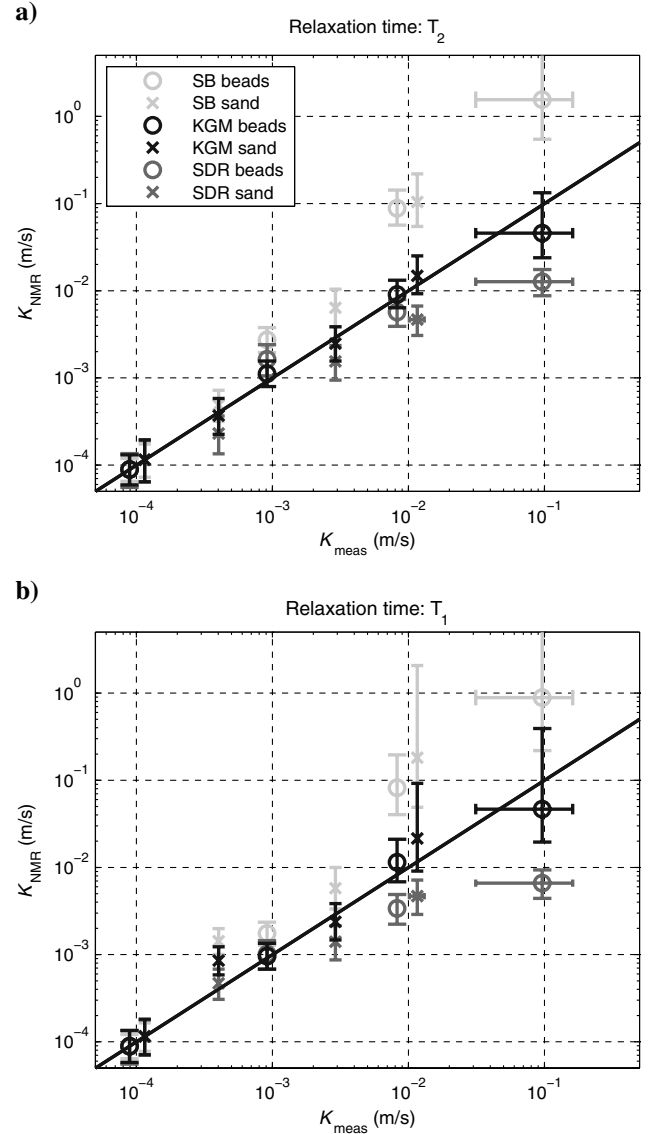
Figure 5. The difference between KGM for surface relaxivities 35 μm/s (a) and 55 μm/s (b) and Seevers considering T_B (SB) and SDR neglecting T_B. The respective estimated K_{meas} and T_2-relaxation times measured on sand and glass beads for comparison. Error bars smaller marker size are not shown.

Figure 6. Comparison of K_{meas} measured on quartz sand and glass bead and K_{NMR} estimated using the Seevers equation (SB), KGM, and SDR for T_2 (a) and T_1 (b). The sample with the shortest T of each material was used for calibration. Error bars smaller marker size are not shown.

Additionally, one cannot exclude that multiexponential signals may also be due to other effects like nonhomogeneous distribution of surface relaxivities. An assumption for the governing NMR models (Seevers, 1966; Brownstein and Tarr, 1979; Godefroy et al., 2001b) is that the relaxation of the protons at the pore surface is homogeneous for the whole sample, i.e., it can be described by a constant ρ. Small-scale variation of ρ within the diffusion length of a water molecule, $\approx\sqrt{4DT}$ (Woessner, 1963), are averaged and the relaxation process is effectively dominated by a mean surface relaxivity (Foley et al., 1996). For the effect of a spatial distribution of ρ on NMR measurements, see Grunewald and Knight (2011). In this work, ρ is considered to be independent on frequency and temperature, which might be an issue if measurements conducted under diverging conditions are compared. Note, for material with a distribution of pore radii, the coupling of pores become important, i.e., the diffusion of a proton from one pore to another during the relaxation is relevant (Ramakrishnan et al., 1999). Because pore coupling is not considered, samples with a distribution of pore radii are not covered by KGM.

CONCLUSIONS

A new model, the KGM, has been presented and evaluated for predicting K of unconsolidated material including coarse grains, but limited to a narrow pore size distribution. KGM is in good agreement with the commonly used fast-diffusion approximations, e.g., Seevers or SDR equation for fine-grained material. KGM allows for improved prediction of K compared to SDR and Seevers for coarse-grained material by including slow-diffusion case and bulk water relaxation. At least for the presented samples, SDR and Seevers fail to predict K for grain sizes larger than medium sand.

The model replaces the empirical calibration factors by intrinsic NMR parameters (surface relaxivity, bulk-water relaxation time), structural parameter (tortuosity), and physical parameters (self-diffusion constant, dynamic viscosity, density, gravity acceleration). This improves the quality of K predicted from NMR measurements because the calibration with flow measurements focuses on the matrix-specific parameters and therefore increases the range of validity. The presented measurements of K and T on glass beads and quartz sands confirm KGM. Because the estimation of surface relaxivities from K and T using KGM does not account for surface roughness, we refer to apparent surface relaxivities as intrinsic NMR parameter combining surface relaxivity and roughness. We found values of $\approx 55(37)$ μm/s for glass beads and $\approx 35(30)$ μm/s for sand $T_2(T_1)$. Extensive laboratory measurements on different geologic material may narrow the range of apparent surface relaxivities and thus the range for predicted K using KGM without calibration.

The prediction of K using KGM is right now limited to (1) materials with a small range of pore sizes due to the limitation on estimating a single representative T and (2) simple pore geometries like tube-shape, planar, or spherical pores.
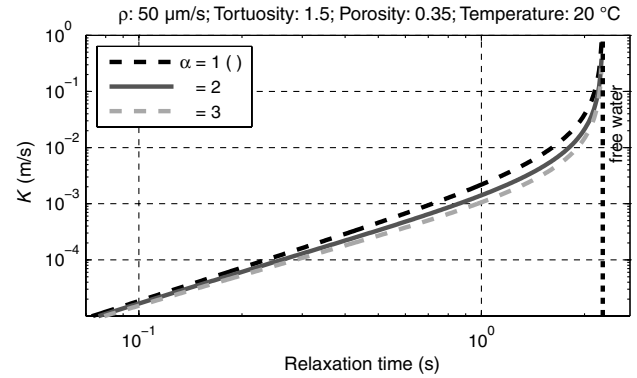
ACKNOWLEDGMENTS

Figure A-1. Comparison of the impact of different pore geometries on KGM, where $\alpha = 1, 2, 3$ for planar, cylindrical, and spherical pores, respectively.

APPENDIX A

KGM FOR PLANAR AND SPHERICAL PORE GEOMETRIES

The governing equations of KGM to describe the fluid flow (equation 1) and the NMR relaxation time (equation 7) can be adapted using an equivalent S/V or are described for other basic pore geometries (Godefroy et al., 2001b). This leads to

$$K = \frac{\varrho g}{2\tau^2\alpha^2\eta}\Phi\left(\frac{-D}{\rho} + \sqrt{\left(\frac{D}{\rho}\right)^2 + \frac{2\alpha DT_BT}{T_B - T}}\right)^2, \quad \text{(A-1)}$$

where $\alpha = 1, 2, 3$ for planar, cylindrical, and spherical pores, respectively. The impact on KGM is shown in Figure A-1. Changes in α do not only lead to a small shift in the predicted K, which can be compensated to some degree by adapting τ, but predominantly affect the range of the slow-diffusion case, which increases with increasing α.

For the presented data sets of glass beads and quartz sand, tube-shaped pores ($\alpha = 2$) work best to find a constant material-specific ρ_a for all samples. For glass beads, a spherical pore geometry ($\alpha = 3$) might also explain the measurements within the error level, but the ranges of ρ_a for the different grain sizes overlap to a lesser degree. Planar pore geometry fails due to the reduced impact of the diffusion. Further research might show if equation A-1 can be successfully applied on samples with other pore geometries.

REFERENCES

Akbar, M., M. Petricola, and M. Watfa, 1995, Classic interpretation problems: Evaluating carbonates: Oilfield review: Schlumberger, **7**, 38–57.

Bartell, F. E., and H. J. Osterhof, 1928, The pore size of compressed carbon and silica membranes: Journal of Physical Chemistry, **32**, 1553–1571, doi: 10.1021/j150292a012.

Bloch, F., 1946, Nuclear induction: Physical Review, **70**, 460–474, doi: 10.1103/PhysRev.70.460.

Bloembergen, N., E. M. Purcell, and R. V. Pound, 1948, Relaxation effects in nuclear magnetic resonance absorption: Physical Review, **73**, 679–712, doi: 10.1103/PhysRev.73.679.

Brownstein, K. R., and C. E. Tarr, 1979, Importance of classical diffusion in NMR studies of water in biological cells: Physical Review A, **19**, 2446–2453, doi: 10.1103/PhysRevA.19.2446.

Carman, P. C., 1938, The determination of the specific surface of powders: Journal of the Society of Chemical Industry, **57**, 225–234.

Carman, P. C., 1956, Flow of gases through porous media: Academic Press.

Carr, H. Y., and E. M. Purcell, 1954, Effects of diffusion on free precession in nuclear magnetic resonance experiments: Physical Review, **94**, 630–638, doi: 10.1103/PhysRev.94.630.

Carrier, W. D., 2003, Goodbye, Hazen; hello, Kozeny-Carman: Journal of Geotechnical and Geoenvironmental Engineering, **129**, 1054–1056, doi: 10.1061/(ASCE)1090-0241(2003)129:11(1054).

Coates, G. R., and J. L. Dumanoir, 1973, A new approach to improved log-derived permeability: SPWLA 14th Annual Logging Symposium, 28.

Dunn, K. J., D. J. Bergman, and G. A. Latorraca, 2002, Nuclear magnetic resonance, petrophysical and logging applications, *in* K. Helbig, and S. Treite, 1st ed.: Pergamon.

Foley, I., S. A. Farooqui, and R. L. Kleinberg, 1996, Effect of paramagnetic ions on NMR relaxation of fluids at solid surfaces: Journal of Magnetic Resonance, Series A, **123**, 95–104, doi: 10.1006/jmra.1996.0218.

Godefroy, S., M. Fleury, F. Deflandre, and J.-P. Korb, 2001a, Temperature effect on NMR surface relaxation: SPE Annual Technical Conference and Exhibition, 13.

Godefroy, S., J. Korb, M. Fleury, and R. Bryant, 2001b, Surface nuclear magnetic relaxation and dynamics of water and oil in macroporous media: Physical Review E, **64**, 1–13, doi: 10.1103/PhysRevE.64.021605.

Grunewald, E., and R. Knight, 2011, A laboratory study of NMR relaxation times in unconsolidated heterogeneous sediments: Geophysics, **76**, no. 4, G73–G83, doi: 10.1190/1.3581094.

Howard, J. J., W. E. Kenyon, and C. Straley, 1993, Proton magnetic resonance and pore size variations in reservoir sandstones: SPE Formation Evaluation, **8**, 194–200, doi: 10.2118/20600-PA.

Hürlimann, M. D., K. Helmer, L. Latour, and C. Sotak, 1994, Restricted diffusion in sedimentary rocks. Determination of surface-area-to-volume ratio and surface relaxivity: Journal of Magnetic Resonance, Series A, **111**, 169–178, doi: 10.1006/jmra.1994.1243.

Josh, M., L. Esteban, C. D. Piane, J. Sarout, D. Dewhurst, and M. Clennell, 2012, Laboratory characterisation of shale properties: Journal of Petroleum Science and Engineering, **88–89**, 107–124, doi: 10.1016/j.petrol.2012.01.023.

Kenyon, W., P. Day, C. Straley, and J. Willemsen, 1988, A three-part study of NMR longitudinal relaxation properties of water-saturated sandstones: SPE Formation Evaluation, **3**, 622–636, doi: 10.2118/15643-PA.

Kenyon, W. E., 1997, Petrophysical principles of applications of NMR logging: The Log Analyst, **38**, 21–43.

Kenyon, W. E., J. J. Howard, A. Sezginer, C. Straley, A. Matteson, K. Horkowitz, and R. Ehrlich, 1989, Pore-size distribution and NMR in microporous cherty sandstones: Proceedings of the 40th Annual Logging Symposium, 24.

Kestin, J., M. Sokolov, and W. A. Wakeham, 1978, Viscosity of liquid water in the range −8°C to 150°C: Journal of Physical and Chemical Reference Data, **7**, 941–948, doi: 10.1063/1.555581.

Kleinberg, R. L., S. A. Farooqui, and M. A. Horsfield, 1993, T1/T2 ratio and frequency dependence of NMR relaxation in porous sedimentary rocks: Journal of Colloid and Interface Science, **158**, 195–198, doi: 10.1006/jcis.1993.1247.

Kleinberg, R. L., C. Flaum, C. Straley, P. G. Brewer, G. E. Malby, G. Friederich, and J. P. Yesinowski, 2003, Seafloor nuclear magnetic resonance assay of methane hydrate in sediment and rock: Journal of Geophysical Research, **108**, 13, doi: 10.1029/2001JB000919.

Kleinberg, R. L., and M. A. Horsfield, 1990, Transverse relaxation processes in porous sedimentary rock: Journal of Magnetic Resonance (1969), **88**, 9–19, doi: 10.1016/0022-2364(90)90104-H.

Kozeny, J., 1927, Über kapillare Leitung des Wassers im Boden: Sitzungsberichte der Akademie der Wissenschaften in Wien, Mathematisch-Naturwissenschaftliche Klasse Abteilung IIa, **136**, 271–306.

Krynicki, K., C. D. Green, and D. W. Sawyer, 1978, Pressure and temperature dependence of self-diffusion in water: Faraday Discussions of the Chemical Society, **66**, 199–208, doi: 10.1039/dc9786600199.

Lanfrey, P.-Y., Z. Kuzeljevic, and M. Dudukovic, 2010, Tortuosity model for fixed beds randomly packed with identical particles: Chemical Engineering Science, **65**, 1891–1896, doi: 10.1016/j.ces.2009.11.011.

Legchenko, A., J.-M. Baltassat, A. Beauce, and J. Bernard, 2002, Nuclear magnetic resonance as a geophysical tool for hydrogeologists: Journal of Applied Geophysics, **50**, 21–46, doi: 10.1016/S0926-9851(02)00128-3.

Mavko, G., and A. Nur, 1997, The effect of a percolation threshold in the Kozeny-Carman relation: Geophysics, **62**, 1480–1482, doi: 10.1190/1.1444251.

McCutcheon, S. C., J. L. Martin, and T. O. J. Barnwell, 1993, Water quality, *in* D. R. Maidment, ed., Handbook of hydrology: McGraw-Hill, 11.1–11.69.

Meiboom, S., and D. Gill, 1958, Modified spin-echo method for measuring nuclear relaxation times: Review of Scientific Instruments, **29**, 688, doi: 10.1063/1.1716296.

Mohnke, O., and U. Yaramanci, 2008, Pore size distributions and hydraulic conductivities of rocks derived from magnetic resonance sounding relaxation data using multi-exponential decay time inversion: Journal of Applied Geophysics, **66**, 73–81, doi: 10.1016/j.jappgeo.2008.05.002.

Pape, H., J. E. Tillich, and M. Holz, 2006, Pore geometry of sandstone derived from pulsed field gradient NMR: Journal of Applied Geophysics, **58**, 232–252, doi: 10.1016/j.jappgeo.2005.07.002.

Ramakrishnan, T. S., L. M. Schwartz, E. J. Fordham, W. E. Kenyon, and D. J. Wilkinson, 1999, Forward models for nuclear magnetic resonance in carbonate rocks: The Log Analyst, **40**, 260–270.

Ronczka, M., M. Müller-Petke, M. Dlugosch, and T. Günther, 2012, A physics-driven approach using single-pore-modes (SPM) for estimating an average pore radius and surface relaxivity from NMR data: Proceedings of the 25th International Conference, SAGEEP, 5.

Seevers, D., 1966, A nuclear magnetic method for determining the permeability of sandstones: 7th Annual Logging Symposium, SPWLA, 1–14.

Straley, C., A. Matteson, S. Feng, L. Schwartz, W. Kenyon, and J. Banavar, 1987, Magnetic resonance, digital image analysis, and permeability of porous media: Applied Physics Letters, **51**, 1146–1148, doi: 10.1063/1.98766.

Timur, A., 1968, An investigation of permeability, porosity, and residual water saturation relationships for sandstone reservoirs: The Log Analyst, **IX**, 8–17.

Whittall, K. P., M. J. Bronskill, and R. Henkelman, 1991, Investigation of analysis techniques for complicated NMR relaxation data: Journal of Magnetic Resonance (1969), **95**, 221–234, doi: 10.1016/0022-2364(91)90213-D.

Woessner, D. E., 1963, NMR spin-echo self-diffusion measurements on fluids undergoing restricted diffusion: Journal of Physical Chemistry, **67**, 1365–1367, doi: 10.1021/j100800a509.